

## Optimization of Density and Radiated Power Evolution Control using Magnetic ELM Pace-making in NSTX

J.M. Canik<sup>1</sup>, R. Maingi<sup>1</sup>, A.C. Sontag<sup>1</sup>, R.E. Bell<sup>2</sup>, D.A. Gates<sup>2</sup>, S.P. Gerhardt<sup>2</sup>, H.W. Kugel<sup>2</sup>, B.P. LeBlanc<sup>2</sup>, J.E. Menard<sup>2</sup>, S.F. Paul<sup>2</sup>, S.A. Sabbagh<sup>3</sup>, V.A. Soukhanovskii<sup>4</sup>  
(email: canikjm@ornl.gov)

<sup>1</sup> Oak Ridge National Laboratory, Oak Ridge, TN 37831

<sup>2</sup> Princeton Plasma Physics Laboratory, Princeton University, Princeton, NJ 08543

<sup>3</sup> Columbia University, New York, NY 10027

<sup>4</sup> Lawrence Livermore National Laboratory, Livermore, CA 94551

### Abstract

Recent experiments at the National Spherical Torus Experiment (NSTX) have shown that lithium coating of the plasma facing components leads to improved energy confinement, and also the complete suppression of edge-localized modes (ELMs). Due to the lack of ELMs, however, such plasmas suffer from density and radiated power that increase throughout the discharge, often leading to a radiative collapse. Previous experiments have shown that ELMs can be controllably restored into these lithium-conditioned discharges using 3D magnetic perturbations, which reduces impurity accumulation. The use of magnetic ELM pace-making has been optimized to control the evolution of the density and impurity content. Short duration large amplitude 3D field pulses are used, so that the threshold field for destabilization is reached and ELMs triggered quickly, and the field is then removed. A second improvement was made by adding a negative-going pulse to each of the triggering pulses to counteract the vessel eddy currents and reduce time-averaged rotation braking. With these improvements to the triggering waveform, the frequency of the triggered ELMs was increased to over 60 Hz, reducing the average ELM size. The optimum frequency for attaining impurity control while minimizing energy confinement reduction was determined: fairly low frequency ELMs (20 Hz triggering) are sufficient to keep the total radiation fraction below 25% throughout the discharge and avoid radiative collapse, with little reduction in the plasma stored energy. When combined with improved particle fueling, the ELM-pacing technique has been successful in achieving stationary conditions in the line-averaged electron density and total radiated power.

### 1. Introduction

The high confinement (H-mode) regime of tokamak operation is characterized by steep temperature and density gradients at the plasma edge, known as the pedestal [1]. While the increased edge pressure leads to significant improvement to energy confinement and global stability, the transport and stability properties of the pedestal pose unique challenges to the operation of future large, near-steady state experiments. A primary concern is that the large pressure gradient at the plasma edge, combined with the large self-driven bootstrap current, typically destabilizes edge-localized modes (ELMs) [2,3], which could severely limit the lifetime of plasma facing components (PFCs). However, these instabilities also tend to flush impurities from the plasma, so that sufficient purity and stationary conditions can be maintained [4]. In ELM-free H-modes, if enhanced particle transport is not achieved, particle transport is quite small with heavy impurities tending to be convected into the plasma [5], so that the plasma density and radiated power ramp, and steady state conditions are unachievable.

In this paper we present results of experiments conducted on the National Spherical Torus Experiment (NSTX), in which three-dimensional (3D) magnetic fields are used to control these two aspects of ELMs in order to improve discharge evolution. Similar 3D perturbations have previously been used on other experiments to suppress [6] or mitigate [7] ELMs. On NSTX, however, it has been found that applying these 3D fields destabilizes ELMs [8]. Making use of this effect, the perturbations have been applied to 1) increase the ELM frequency and reduce the energy expelled during each event, and 2) provide a mechanism for controlling the density and radiation evolution during plasmas with lithium-coated PFCs. The use of lithium in these experiments eliminates natural ELMs [9], making the plasma susceptible to strong impurity accumulation.

## 2. ELM destabilization with 3D field application with lithium coated PFCs

The NSTX plasmas studied in these experiments had major and minor radii of 0.85 and 0.6 m, respectively, elongation of  $\kappa=2.4-2.6$ , and triangularity  $\delta=0.7-0.8$ . The boundary was near-double-null biased slightly to the lower X-point ( $dr^{\text{sep}}$ —the distance between the primary and secondary separatrices at the outboard midplane—was  $\sim 5$  mm), with the ion grad-B drift direction favorable for H-mode access. The toroidal magnetic field was  $B_t=0.45$  T, the plasma current was 800 kA, and all discharges were heated with 4 MW of neutral beam injection. 3D fields are applied during NSTX plasma using a single row of six coils located at the plasma midplane [10], configured to produce an  $n=3$  perturbation in the experiments described here. These coils produce a fairly broad spectrum, as shown in Figure 1. As a result, significant resonant components exist over a broad region of the plasma edge, sufficient to stochastize the pedestal if not screened, as described in ref [11]. Details of ELM destabilization with boronized carbon PFCs have been presented previously [8,11]; here we focus on results using lithium coated PFCs.

The destabilization of ELMs by applying 3D fields is illustrated in Figure 2, where  $n=3$  fields of varying amplitudes are applied in a sequence of discharges. Since heavy lithium coatings were applied to the PFCs during these discharges, the control discharge without applied fields (the midplane array was used to correct known error fields only) was ELM-free (panel a). A current of 500 A in the  $n=3$  field was insufficient to trigger ELMs (panel b), whereas destabilization was observed at 750 A (panel c). At a higher current of 1 kA, the period between triggered ELMs was reduced (panel d).

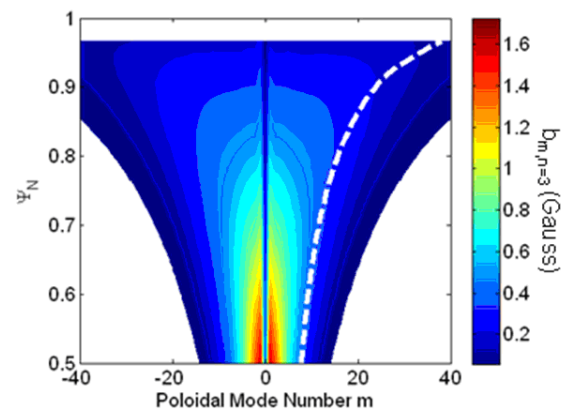


FIG 1: Poloidal spectrum of the applied  $n=3$  perturbation

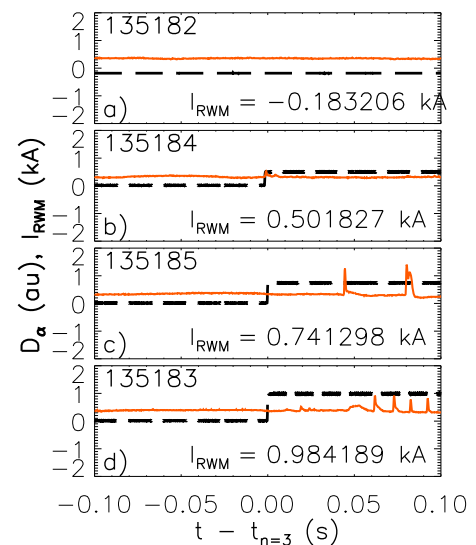


FIG 2:  $D_\alpha$  time traces (red) as  $n=3$  fields amplitude (dashed black) is increased.

Previous experiments studying the effects of 3D fields on ELM stability in NSTX showed that, with boronized carbon PFCs, the 3D field application led to an increase in the pedestal electron temperature [8]. This gave a higher maximum pedestal pressure gradient, which was calculated to degrade the stability to edge modes, consistent with observation. This effect of the 3D fields was not observed with lithium coatings applied to the PFCs. Under these conditions, the  $n=3$  field leads to a flattening in both the electron density and temperature at a radius of  $\psi_N \sim 0.8-0.9$ , as shown in Figure 3. The gradients in the main part of the pedestal outside of  $\psi_N \sim 0.9$  are largely unaffected, and the increase in temperature seen with boronized PFCs is not observed with lithium. A local minimum in the toroidal rotation ( $V_{\text{tor}}$ ) is also observed which is in the same region as the flattening in the electron profiles, suggestive of island formation.

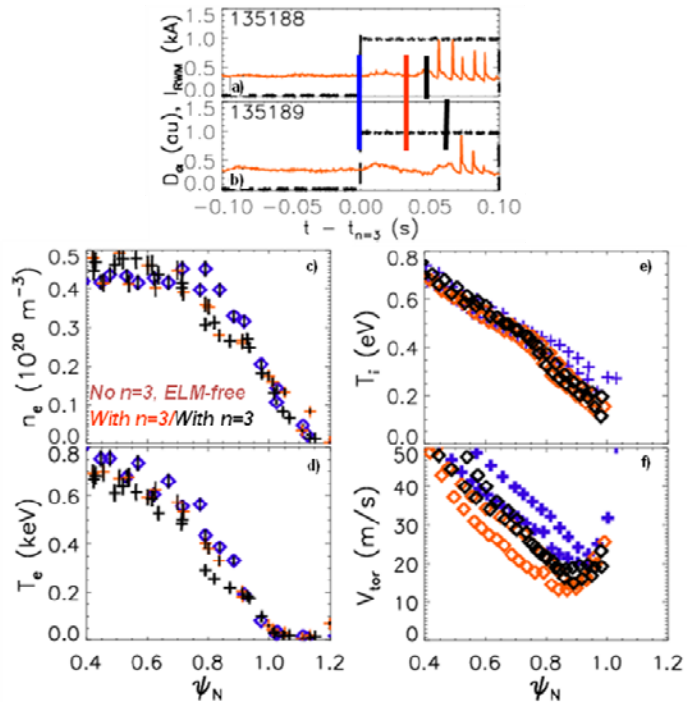


FIG 3: a), b) time traces marking points of profile measurements and profiles of electron c) density and d) temperature, e) ion temperature and f) toroidal rotation. Time slices from before (blue)  $n=3$  field turn-on, 33 ms after turn-on (red), and just prior to ELM onset (black)

The lack of steepening in the pedestal electron pressure profiles with lithium coated PFCs leaves the underlying cause of the change in ELM stability with applied  $n=3$  fields unclear. Two possible explanations that can be considered are the effects of toroidal rotation on peeling-ballooning stability, and possible changes to the stability boundary itself caused by the  $n=3$  fields. Calculations with the ELITE code for MAST plasmas have shown that toroidal rotation can have a stabilizing effect on peeling-ballooning modes [12]; conversely the reduced edge rotation with  $n=3$  fields in NSTX could lead to the observed reduced ELM stability. Alternatively, the 3D nature of the plasma equilibrium with the  $n=3$  fields applied may alter the stability properties even for fixed plasma profiles, so that the standard 2D codes cannot accurately describe stability. However, while both of these effects may have a strong impact on growth rates at fixed pressure and current, neither is expected to substantially alter instability onset conditions. In contrast, the plasma is calculated to lie quite far from the peeling-ballooning stability boundary in lithium conditioned plasmas [9], requiring that the departure from the conventional 2D theory be quite strong to explain the altered ELM stability in experiments. Quantification of these effects on the theoretical edge stability of NSTX plasmas is a focus of present research.

### 3. Optimization of ELM pacing by applied $n=3$ fields

The experiments described in the previous section made use of static  $n=3$  fields to destabilize ELMs. However, the relatively large perturbations required to trigger ELMs result in strong braking of the plasma rotation by neoclassical toroidal viscosity [13], degrading the global stability of the plasma. To mitigate the effects on rotation, pulsed  $n=3$  fields were used during ELM pacing experiments, where the triggering effect of the applied fields was used to increase the ELM frequency. This technique is of general interest for future toroidal confinement devices operating in the H-mode, since it may be a means by which the size of ELMs can be controlled. Magnetic ELM pacing has another primary purpose in NSTX: the control of particle and impurity content in plasma discharges with lithium coated PFCs. As shown previously, these coatings eliminate ELMs, which leads to difficulty with uncontrolled rise of the density and radiated power, typical in the ELM-free H-mode.

To perform ELM pacing using pulsed  $n=3$  fields, the waveform of the applied perturbation was optimized [14]. The goals of this optimization were to increase the ELM frequency as much as possible while minimizing the damping of toroidal plasma rotation. The latter is essentially a requirement to minimize the time-averaged applied fields. These requirements favor the use of pulsed fields rather than DC, each pulse tailored to trigger a single ELM. The rotation was then allowed to recover between pulses, so that the deleterious effects of low rotation on plasma stability could be largely avoided. It was observed that the time delay between  $n=3$  turn-on and ELM onset was reduced as the pulse amplitude was increased. By maximizing the  $n=3$  field during the pulses, ELMs could be triggered very rapidly and so the ELM frequency increased. The final optimization of the triggering waveform was to add brief secondary pulses with opposite polarity to the triggering pulses, in order to counteract vessel eddy currents induced by the ex-vessel coils and more quickly remove the perturbing fields from the plasma. These negative-going spikes were successful in reducing the time-averaged perturbation inside the vacuum vessel, and maintaining high rotation during the ELM paced discharges, as illustrated in Figure 4.

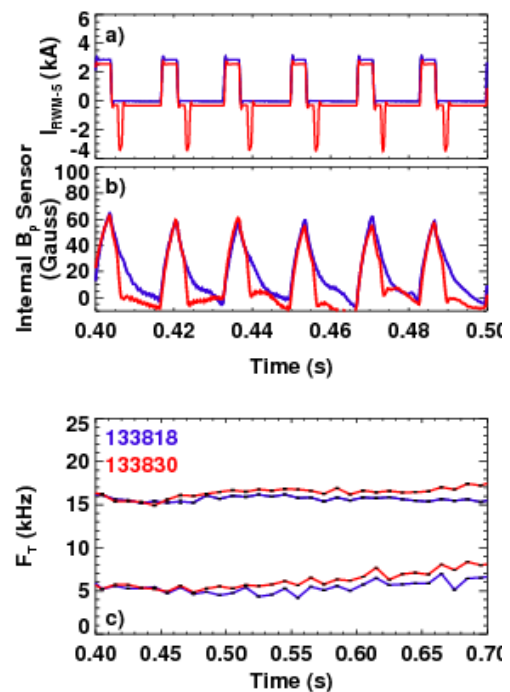


FIG 4: Time traces of a)  $n=3$  pulses in ex-vessel coils, b) magnetic field measured inside vessel, and c) toroidal rotation at two radial locations for pulses without (blue) and with (red) negative-going trailing pulses

In addition to the optimizations to the triggering waveform, the effectiveness of ELM pacing in reducing impurity buildup and ELM size was evaluated as a function of triggering frequency. This frequency optimization was performed using unipolar pulses, as this was executed before the waveform was tailored with negative-going trailing pulses. As shown in Figure 5, performing ELM pacing reduced the density and radiated power rise at all frequencies compared to the ELM-free control case. The carbon content and  $Z_{\text{eff}}$  of the plasma was reduced as well, indicating a reduction in the low-Z impurities and improved purity (the radiation is dominated by metallic impurities [15]).

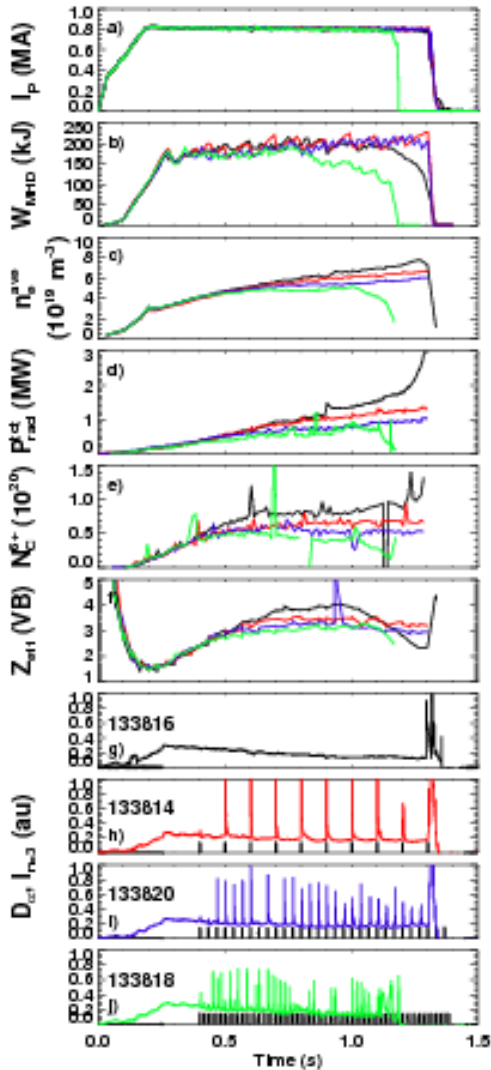


FIG 5: Time traces as ELM frequency is increased of a) plasma current, b) stored energy, c) line-average electron density, d) radiated power, e) total carbon content, f) average  $Z_{\text{eff}}$ , and g-j)  $n=3$  field and  $D_{\alpha}$

#### 4. Towards fully arresting the density and radiated power evolution

The primary goal of performing ELM pacing during NSTX discharges with lithium coated PFCs is to provide full control over the density and radiated power evolution. This has been proposed as a new high-performance plasma scenario: lithium coatings are used to improve energy confinement, and pacing is used to eliminate the impurity buildup that tends to occur due to the lack of natural ELMs [8]. To improve the particle control in this scenario, experiments were performed

These improvements are largely present even for low triggering frequencies of 10-20 Hz, as shown in Figure 6. While the reduction in impurities is larger for higher frequencies, the energy confinement is degraded as well, with a  $\sim 10\%$  reduction in plasma stored energy at a triggering frequency of 60 Hz. Thus, fairly modest ELM frequency is sufficient for preventing radiation runaway and improving plasma purity, while minimizing the penalty in energy confinement. However, from the standpoint of controlling the ELM size, maximizing the frequency is desired. Both the average ELM size (as quantified by the average  $\Delta W/W$ , where  $W$  is the stored energy before an ELM, and  $\Delta W$  is the energy expelled by the ELM), and also the maximum energy (average  $\Delta W/W$  of the largest 20% of ELMs) are reduced as the frequency is increased. At the highest triggering frequency of 60 Hz, the average ELM size is reduced to  $\Delta W/W \sim 5\%$ , and the largest ELMs are reduced to  $\Delta W/W \sim 10\%$ , compared to 15 and 20%, respectively, at 10 Hz triggering frequency. Even at the highest frequency ELM size remains too large to be tolerable in future large devices; further increase in the ELM frequency is needed, which may require in-vessel coils.

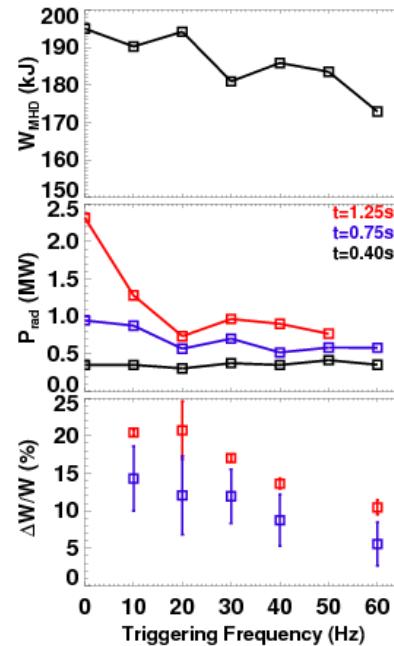


FIG 6: Dependence of a) stored energy, b) radiated power, and c) average ELM size (blue) and mean of largest 20% of ELMs (red) on triggering frequency

combining ELM pacing with improved gas fueling of the plasma discharge. Although the density can be reduced even at low triggering frequencies, these experiments used the highest frequencies achievable in order to maximize the particle expulsion.

NSTX plasmas are typically partially fueled using a gas puff located on the center column of the torus. This location is chosen since high field side fueling has been shown to ease H-mode access in spherical torii [16,17]. However, due to restricted access on the center post, this system is limited to rather slow time response in the particle input. Gas is introduced early to assist fueling during the plasma startup, and then remains on, such that substantial fueling persists throughout the plasma current flat-top. In order to reduce this unneeded fueling during the majority of the discharge, the gas input during startup was improved using a supersonic gas injector (SGI) [18]. This injector can rapidly switched on and off during the discharge, giving better control of the fueling evolution throughout the discharge phases. The injector can also be placed close to the plasma edge, and has higher fueling efficiency than other available fast gas valves. By partially replacing fueling from the center stack valve with the SGI, the particle input during the plasma flat-top can be reduced. In the experiments described here, this approach was successful in reducing the gas input from the center column by  $\sim 30\%$ .

The improved fueling was combined with ELM triggering to both reduce particle input during flat-top and increase the effective particle transport through the pedestal. The waveform of the applied  $n=3$  fields used during these experiments included the negative-going trailing pulses described above, so that high frequency triggering could be applied while minimizing the impact on toroidal rotation. Time traces from a discharge combining SGI and ELM pacing are shown in Figure 7, along with data from a discharge with SGI fueling only. In the case with pacing, when ELMs begin at  $t \sim 0.4$  s the line-averaged electron density ceases ramping and becomes quasi-stationary, showing that the combination of improved fueling and pacing has successfully provided effective particle control. A similar behavior is observed in the total radiated power, which is nearly constant once the ELM pacing begins. This period of quasi-stationary line-averaged density and total radiated power lasts for  $\sim 300$  ms ( $\sim 7$  energy confinement times), at which point a rotating MHD mode appears that appears to be a  $2/1$  neoclassical tearing mode (NTM). These modes are common late in NSTX discharges [19], and are not unique to cases with applied 3D fields.

These periods of quasi-stationary global conditions achieved by this technique show the proof-of-principle that ELM pacing is effective for particle control with lithium-coated PFCs. However, the radial profiles of the plasma parameters are not

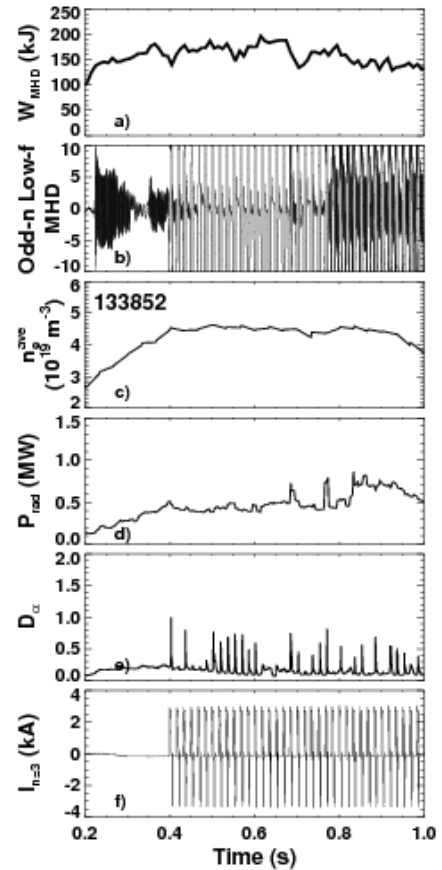


FIG 7: Time traces of a) stored energy, b) odd- $n$  magnetic activity, c) line-average electron density d) radiated power, e)  $D_\alpha$  and f)  $n=3$  field current using combined SGI and ELM pacing

stationary during these phases. In particular, the edge densities—including electron, local radiated power, and carbon—show a decrease in time during the ELM pacing phase, and the core densities increase [14]. This is illustrated in Figure 8, which shows the electron density and temperature profiles from a time slice just before the ELM pacing begins, and late in the pacing phase (but before onset of the mode described above). The reduction in the edge density combined with the rising core value leads to a stronger peaking of the density profile. This carries over into the electron pressure profile, so that the core pressure gradient is larger when ELM pacing is performed. The higher gradient may play a role in the apparent 2/1 NTM onset by providing a stronger drive for the instability. In addition, the  $n=3$  fields slow rotation, reducing the stabilizing effects. Finally, the presence of large ELMs during this phase provides many opportunities for triggering the NTM, as has previously been observed on NSTX for natural ELMs [19]. The combination of these effects may make the plasma more prone to these  $n=1$  modes, which are often observed during high frequency pacing experiments (as well as in non-paced experiments).

## 5. Discussion and future directions

ELMs can be destabilized by the application of 3D fields in NSTX H-mode discharges under many conditions, in particular during ELM-free H-modes induced by lithium coatings on the PFCs. This effect has been used as an ELM pacing technique, with several optimizations performed in order to maximize the frequency of ELMs triggered by 3D fields. In addition to reducing ELM size, the ELM pacing technique has been employed to reduce the impurity accumulation and aid density control during lithium conditioned discharges. This has been successful, when combined with improved fueling control using an SGI, in providing periods of quasi-stationary line-averaged density and total radiated power.

However, further development is needed in order to improve the ELM pacing technique for providing particle control during high-performance plasmas. First, although the global parameters can be arrested at high triggering frequency, the plasma profiles continue to evolve. In particular, the core electron, radiation, and carbon densities show a secular increase during ELM paced shots that is similar to discharges without ELM pacing; while edge control is achieved, the core remains problematic. To overcome this, the core particle and impurity transport must be increased in conjunction with the ELM pacing. One possible method for achieving this increase may be through the application of RF heating of the core plasma. This has been shown in other toroidal experiments to often mitigate the accumulation of high-Z impurities [20]. Experiments to test this idea using the NSTX high harmonic fast wave heating system are planned.

The frequent occurrence of  $n=1$  rotating MHD modes is a second area of concern for the future application of ELM pacing for impurity control. As described above, several

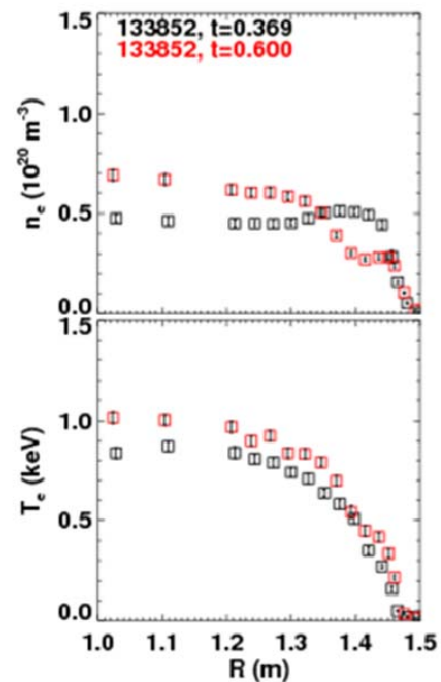


FIG 8: Profiles early (black) and late (red) in the ELM pacing phase

features of the ELM-paced discharges may combine to make the plasma more prone to these modes. However, the use of RF heating to increase core particle transport may offer a solution to this aspect as well. If this is successful in reducing the core density, then the pacing should be sufficient at a lower frequency, since it is not necessary to reduce the edge density in time as has been done in the experiments described here. The reduced ELM frequency, combined with reduced peaking of the density and pressure profiles, may be sufficient to avoid triggering the  $n=1$  modes.

This research was sponsored in part by U.S. Dept. of Energy Contracts DE-AC05-00OR22725, DE-AC02-09CH11466, DE-AC52-07NA27344, and DE-FC02-04ER54698. The authors would also like to thank the NSTX technical and operations staff for their support of this research.

## References

- [1] F. Wagner, *Plasma Phys. Contr. Fus.* **49** (2007) B1.
- [2] H. Zohm, *Plasma Phys. Control. Fusion* **38** (1996) 105.
- [3] P.B. Snyder *et al*, *Phys. Plasmas* **9** (2002) 207.
- [4] D.N. Hill, *J. Nucl. Mat.* **241-243** (1997) 182.
- [5] T. Putterich *et al*, 36<sup>th</sup> EPS Conf. on Plasma Phys., Sofia, Bulgaria, June 29-July 3, 2009, ECA Vol. 33E, P-1.158 (2009).
- [6] T. E. Evans, *et al*, *Phys. Rev. Lett.* **92** (2004) 235003.
- [7] Y. Liang *et al*, *Phys. Rev. Lett.* **98** (2007) 265004.
- [8] J.M. Canik *et al*, *Phys. Rev. Lett.* **104** (2010) 045001.
- [9] R. Maingi *et al*, *Phys. Rev. Lett.* **103** (2009) 075001.
- [10] A.C. Sontag *et al*, *Phys. Plasmas* **12** (2005) 056112.
- [11] J.M. Canik *et al*, *Nucl. Fusion* **50** (2010) 034012.
- [12] S. Saarelma *et al*, *Plasma Phys. Contr. Fusion* **49** (2007) 31.
- [13] W. Zhu *et al*, *Phys. Rev. Lett.* **96** (2006) 225002.
- [14] J.M. Canik *et al*, *Nuc. Fusion* **50** (2010) 064016.
- [15] S. Paul *et al*, *J. Nucl. Mat.* **390-391** (2009) 211.
- [16] A.R. Field *et al*, *Plasma Phys. Contr. Fusion* **44** (2002) A113.
- [17] R. Maingi *et al*, *Nucl. Fusion* **43** (2003) 969.
- [18] V.A. Soukhanovskii *et al*, *Rev. Sci. Instrum.* **75** (2004) 4320.
- [19] S.P. Gerhardt *et al*, *Nucl. Fusion* **49** (2009) 032003.
- [20] O. Gruber *et al*, *Nucl. Fusion* **49** (2009) 115014.